UNIVERSITY OF CRETE
MATERIALS SCIENCE AND TECHNOLOGY DEPARTMENT

Microfluidics in biomaterials for bone tissue engineering applications

Eleftheria Babaliari

Supervisor: Prof. M. Chatzinikolaidou
co supervisors: Prof. G. Petekidis, Prof. M. Vamvakaki

Dept. of Materials Science and Technology, University of Crete, Heraklion
&
Foundation for Research and Technology, Hellas (FORTH)
Institute of Electronic Structure and Laser (IESL)

April 2015

Acknowledgments

I would like to thank my supervisor Prof. Maria Chatzinikolaidou for the time she spent in fruitful discussions with me and all her support, Prof. George Petekidis for his contribution to my rheological background and all his help, Prof. Maria Vamvakaki for her contribution to my committee and Dr. Maria Farsari for the collaboration. I would also like to thank all the members of the biomaterials lab and the polymer group for their assistance, as well as, for the friendly working atmosphere. Finally, I would like to thank my family and my friends for supporting me all these years in all areas.

Contents

1. Introduction

In recent years, the clinical demand for bone grafts is extremely large across the population. However, the limited volume of bone grafts and frequent morbidity of patients leads to the need for the development of advanced therapeutic strategies for bone regeneration. Tissue engineering has emerged as a promising field for the development of new bone graft substitutes in order to overcome the limitations of the current grafts. However, besides the selection of the biomaterial and the cell source, several other issues should be considered, including the optimization of the *in vitro* culturing system.

Cells in a multicellular organism live under a considerably different environment compared to conventional static cultures. They are attached to much softer materials than the glass and plastic substrates, on which most studies are done in vitro, and are surrounded by fluid and nutrients. Lots of evidence show that physical parameters such as fluid shear, mechanical forces, flexibility and media accessibility can have profound effects on cell growth and differentiation [1].

It has been reported that dynamic culturing of cell - biomaterial constructs has a positive effect on cell proliferation [2-5] and cell differentiation [6]. Moreover, it has been shown that dynamic culture conditions enhance the proliferation and differentiation of pre-osteoblasts [7-10]. Considering this approach crucial for the tissue maturation, and taking into account the dynamic *in vivo* situation, we focused on setting up a new microfluidic system, which together with the development of a biomaterial substrate for the cells, would be appropriate for the investigation of dynamic biological experiments.

Microfluidics reflect more appropriately the in vivo environment of cells in tissues such as the normal fluid flow within the body, consistent nutrient delivery, effective waste removal and mechanical stimulation due to fluid shear forces. Taking account this approach, the objective of the present work was to investigate the effect of dynamic culture on tissue growth together with the use of biomaterial substrates for cells. For this purpose, we firstly set up a new microfluidic system. Fluid flow, which exerts a shear stress on adherent cells, has been identified as one of the strongest stimuli on bone cell behavior. It provides sufficient levels of oxygen and nutrients at the interior of the biomaterials and mechanical stimulation to the cells. Then, in order to enhance initial cell adhesion, as well as, proliferation and differentiation of pre-osteoblastic cells, we coated the inner surface of the microfluidic system with gelatin film and collagen fiber networks. Afterward, we investigated the rheological properties of collagen gel to better understand the mechanical environment of cells. It has been shown that the mechanical properties of the substrate produce a profound impact on cell and tissue behavior [11]. Indeed, the gel elasticity directly influences how cells spread, migrate, contract, organize key extracellular structures such as focal adhesions, as well as, proliferate and differentiate [11-18]. Finally, we studied the

proliferative and osteogenic behavior of pre-osteoblastic cells in dynamic conditions and compared them with static culture conditions.

Therefore, this work may be beneficial as a model system in understanding and developing perfusion culture systems for the future creation of graft substitutes using larger microfluidic devices.

The thesis text in following is structured with a background, an introduction of the experimental methods, a presentation and discussion of our experimental findings and finally with the conclusions.

2. Background

2.1 Microfluidics

Microfluidics is a multidisciplinary field including chemistry, biochemistry, nanotechnology, biotechnology, physics and engineering with applications to the design of systems in which small volumes of fluids will be handled. It deals with the precise control, behavior and manipulation of fluids which are geometrically constrained to a sub-millimeter scale.

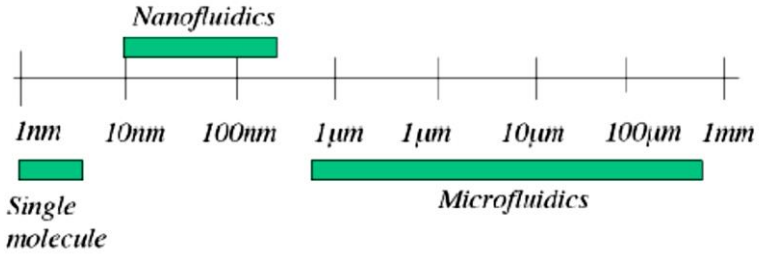

Figure 2.1: *Scale bar of microfluidics* [19].

2.2 Microfluidic cell culture

Microfluidic cell culture controls fluid flow in the micrometer scale in precisely defined geometries and facilitates manipulation and analysis starting from a single cell level, to larger cell populations and up to tissues cultured on fully integrated and automated chips. Microfluidics also provide an extra degree of control over cultured cells by delivering not only chemical but also mechanical signals. Furthermore, using microliter-sized assay chambers results in reduced consumption of costly reagents and increased precision. Finally, microfluidic systems can be automated to an immense extent that allows culturing cells for several weeks under precisely defined conditions without manual intervention [20, 21].

Laminar flow regimes, small length scales and diffusion dominated mass transport characterize the microfluidic devices [22]. These characteristics can be used to provide a biomimetic environment for cell and tissue culture, and consequently advance conventional static culture with the creation of unique environments that mimic the intracellular environment. Furthermore, laminar flow replicates the normal fluid flow within the body, facilitates mass transport of solutes, and supplies consistent nutrient delivery and effective waste removal resulting in a more *in vivo*-like environment. Indeed, one of the advantages that microfluidics bring to cell culture is the continuous

flow of fresh media within the culture system. Finally, small volumes of media in microfluidic cell culture devices reflect more appropriately the physiological condition of cells in tissues than cells that are cultured in larger volumes due to faster consumption of nutrients and increased concentration of metabolites and secreted molecules, similar to tightly packed tissues (Figure 2.2).

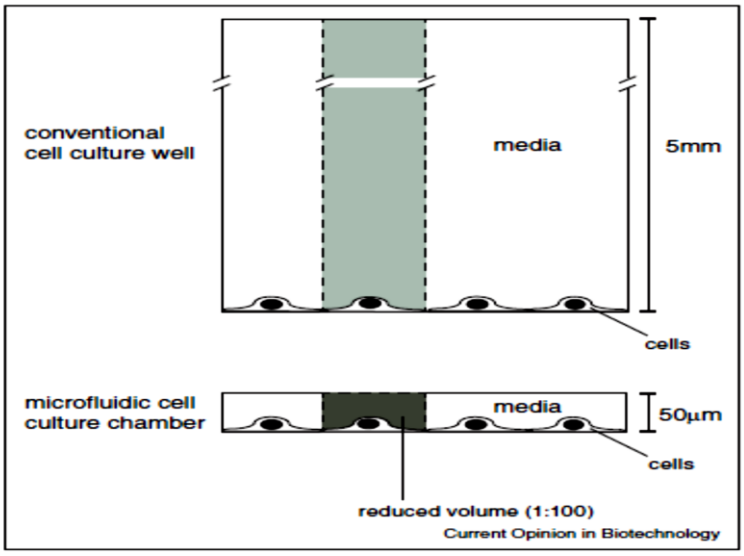

Figure 2.2: *Illustration of 'small-volume-effects' in microfluidic cell culture devices* [23].

2.3 Biomaterials

A biomaterial is a material intended to interface with biological systems to evaluate, treat, augment or replace any tissue, organ or function of the body [24]. It provides a desirable environment for cells for the production of the tissue. Ideally, biomaterials should possess an interconnected pore network to permit cell infiltration, diffusion of nutrients, and removal of wastes. Additionally, they should be fabricated from biocompatible and biodegradable materials, and possess chemical properties to support cell adhesion and sufficient mechanical strength to withstand implantation and in vivo stresses [25, 26].

Both gelatin and collagen are natural biomaterials, biocompatible, biodegradable, easily available and highly versatile. Collagen is the major component of the bone matrix, and a molecule that makes up approximately 30% of all body proteins [27] while gelatin is an irreversibly hydrolyzed form of collagen and its chemical composition is closely similar to that of its parent collagen.

Cells cultured within collagen gels are surrounded by 'native' extracellular matrix (ECM) proteins and can remodel their surrounding fibrous matrix. This remodeling is modulated by local and global physical cues, resulting in changes to the mechanical properties. This 'dynamic reciprocity' between the cells and the matrix resembles that which occurs *in vivo* [28]. Remodeling of ECM [29] is a key aspect of tissue development and fibrosis, is critical for 'functional tissue engineering', and is a major advantage of utilizing the collagen gel model system.

2.4 Characterization of collagen gels

When a cell attaches to a substrate with adhesion molecules on the cell membrane, such as integrins, the cytoskeleton transmits traction forces between the multiple attachment sites, which deform the culture substrate according to its stiffness. In this way, cells can feel the stiffness of their substrates and then respond by remodeling the cytoskeleton and changing the expression of adhesion molecules [12]. Cell-cell adhesion and cell-substrate adhesion are important interactions that modulate intracellular signaling pathways for proliferation and differentiation, as well as, various cellular events from gene expression to cell locomotion [14]. Thus, it is useful to characterize the mechanics of the collagen gels so as to better understand the mechanical environment of the cells and to assess the cell-mediated remodeling and resulting changes in the functional mechanical properties of the more tissue-like material [30].

The mechanical properties of collagen gels depend on many parameters such as collagen density, pH, and temperature [30]. However, we should not forget the profound effects of cell remodeling. Cells profoundly alter their local environment leading to pronounced densification of the surrounding gel which alters mechanical signaling even with low cell density and short culture duration (minutes to hours). With higher cell density and longer culture duration (hours to days), the cells alter the global properties dramatically with greater than 10-fold compaction, reorganization (bundling of fibrils) and cross-linking of fibers.

In the short-term collagen gels can be considered physical gels with few crosslinks and >90% water. In terms of bulk behavior, a collagen gel can be considered an entropic spring such as an elastomeric polymer, being extended from its highest entropy state and losing organizational entropy (and excluding water) when stretched [31].

Many methods have been employed in order to study collagen gel mechanics, such as rheology [30].

2.5 Rheology

Rheology is the study of the flow of matter: either in the liquid state or of 'soft solids'. This applies to substances which have a complex molecular structure, such as suspensions, polymers, body fluids and other biological materials. The flow of these substances cannot be characterized by a single value of viscosity (at a fixed temperature or rate). While the viscosity of liquids normally varies with temperature, in complex soft materials variations with other factors are also of interest. Theoretical aspects of rheology are the relation of the flow/deformation behavior of a material and its internal structure, and the flow/deformation behavior of materials that cannot be described by classical fluid mechanics or elasticity. In practice, soft matter rheology is principally concerned with extending the "classical" disciplines of elasticity and (Newtonian) fluid mechanics to materials whose mechanical behavior cannot be described with the classical theories. It is also concerned with establishing predictions for mechanical behavior (on the continuum mechanical scale) based on the micro- or nanostructure of the material. Materials flow when subjected to a stress, that is a force per area. There are different sorts of stresses (for example shear, torsional) and materials can respond in various ways. Thus, much of theoretical rheology is concerned with the forces associated and external applied loads and stresses, and the resulting internal strains.

When a force is applied to a volume of material (Figure 2.3) then a deformation (D) occurs. If two plates (area A) separated by fluid of thickness H, are moved (at velocity V by a force F) relative to each other, Newton's law states that the shear stress (F/A) is proportional to the shear strain rate (V/H). The proportionality constant is known as the dynamic viscosity η.

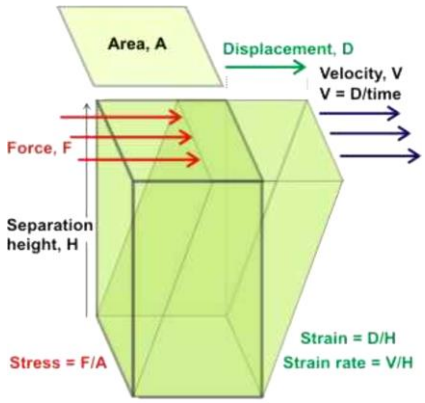

Figure 2.3: *Schematic representation of a sample's deformation* [32].

One way to characterize the rheological response of a system is to measure the shear moduli as a function of frequency (dynamic measurements). In this way in order to explore the rates of structural rearrangement within a complex fluid, a small-

amplitude oscillatory shear is imposed. This kind of deformation can be achieved in a cone and plate geometry by rotating the bottom plate about its axis with an angular velocity that oscillates sinusoidally $\Omega(t) = \Omega\cos(\omega t)$, where ω is the frequency of oscillation, in units of radians per second. The shear rate $\dot{\gamma}$ is a sinusoidal function of time $\dot{\gamma} = \frac{\Omega \cdot r}{h}$ and so is the shear strain $\gamma = \frac{\Omega o \cdot r}{\omega \cdot h} \sin(\omega t) = \gamma_o \sin(\omega t)$. The ratio $\gamma_o = \frac{\Omega o \cdot r}{\omega \cdot h}$ is the strain amplitude. If the strain amplitude γ_o is small enough that the fluid structure is not much disturbed by the deformation, then the stress measured during the oscillatory deformation is controlled by the rates of spontaneous rearrangements, or relaxations present in the fluid in the quiescent or equilibrium state. The shear stress $\sigma(t)$ produced by a small amplitude deformation is proportional to the amplitude of the applied strain γ_o and is itself sinusoidally varying in time. In general, the sinusoidally varying stress can be represented as

$$\sigma(t) = \gamma_o [G'(\omega)\sin(\omega t) + G''(\omega)\cos(\omega t)] \quad \textit{(equation 2.1)}$$

where G' is the storage modulus and G" the loss modulus. The storage modulus represents storage of elastic energy while the loss modulus represents the viscous dissipation of that energy. When the ratio G'/G" is high (>>1) the material has solid-like behavior but if G'/G" is low (<<1) the material has liquid-like behavior.

2.6 MC3T3-E1 pre-osteoblastic cells

The osteoblastic MC3T3-E1 cell line has been derived from mouse C57BL/6 calvaria. The pre-osteoblastic cells are adherent and show a fibroblastic morphology in the growing state. Moreover, they have the capacity to differentiate into osteoblasts and osteocytes and have been shown to form calcified bone tissue in vitro. Mineral deposits have been identified as hydroxyapatite [33, 34]. The main reason that MC3T3-E1 pre-osteoblastic cells were selected as ossification model is the expression of many differentiation markers, such as alkaline phosphatase and collagen.

2.7 Osteogenic markers of MC3T3-E1 cells

2.7.1 Alkaline phosphatase (ALP) activity

Alkaline phosphatase (ALP) is reported to be an early marker of osteoblast differentiation [7]. ALP is an enzyme associated with the formation and calcification of hard tissues [35]. More specifically, ALP is attached to the external surfaces of

plasma membranes by phosphoethanolamine bound to oligosaccharide, which is, in turn, covalently linked to the polar head group of phosphatidylinositol [36-38]. Finally, ALP is released from plasma membranes by phosphatidylinositol-specific phospholipase C (PIPLC) [39-42].

2.7.2 Collagen production

Collagen is the main extracellular protein of bones. Detection of soluble collagen contents in the culture supernatant is useful as differentiation marker. Collagen is composed of a triple helix, which consists of two identical chains and an additional chain that differs slightly in its chemical composition. The chain contains about 1000 amino acid residues and is arranged as a left-handed helix with three amino acid residues per turn with glycine at every third residue. A chain is composed of a series of triplet Gly-Pro-Y, with Y hydroxyproline. Glycine is the only amino acid small enough to occupy the crowded interior of the triple helix [43, 44].

3. Experimental methods

3.1 Microfluidic system

The flow perfusion culture system is composed of a resealable chip interface (Dolomite) (Figure 3.1.A) including the microfluidic devices (Dolomite). The microfluidic devices are composed of a glass base chip for the cell layer and substrate (B) and PMMA chips with PDMS gaskets for loading cells and substrates (C) and for flowing fluids across the cells and substrates (D).

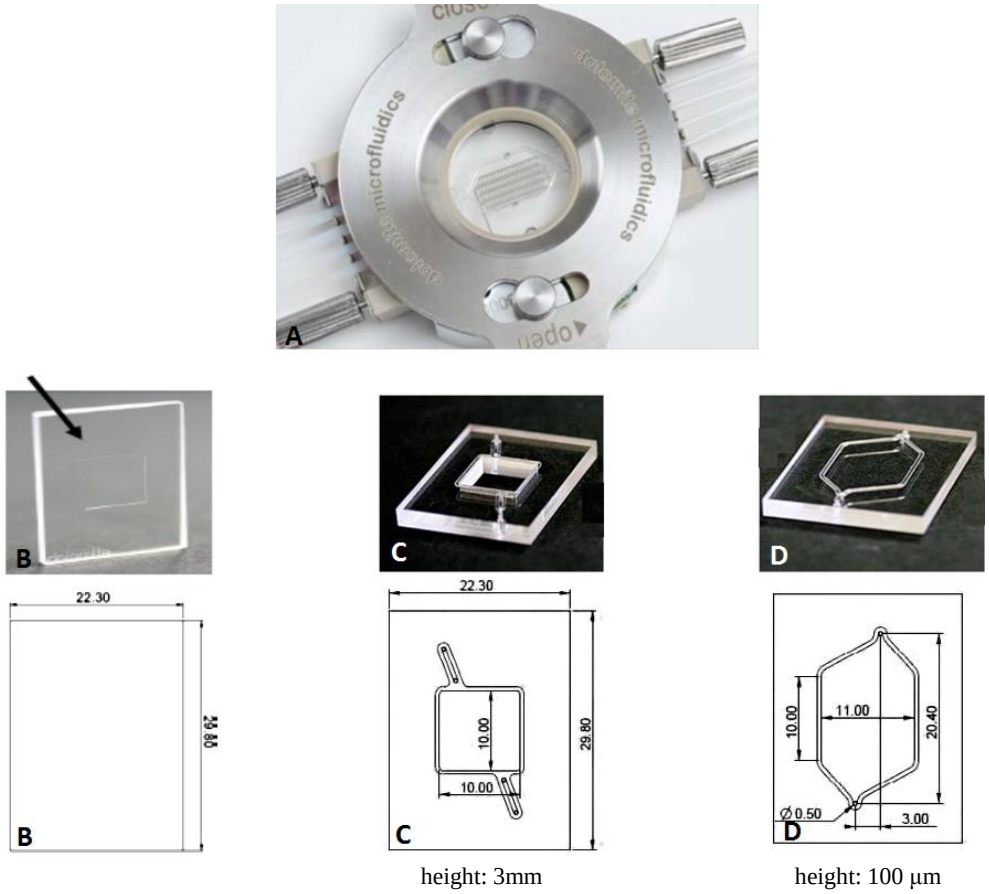

Figure 3.1: *Illustration of the flow perfusion culture system. Dimensions of the microfluidic devices are presented* [45].

More specifically, we insert the glass base chip into the base of the resealable chip interface, we put the PMMA chip with PDMS gasket for loading cells and substrates and finally we close the resealable chip interface (Figure 3.2). Then, we open the resealable chip interface, we take out the PMMA chip with PDMS gasket for loading cells and substrates and we put the PMMA chip with PDMS gasket for flowing fluids across the cells and substrates. The holder then clamps all layers together providing

fluidic connections to the chip with the use of two linear connectors (Dolomite) (Figure 3.3).

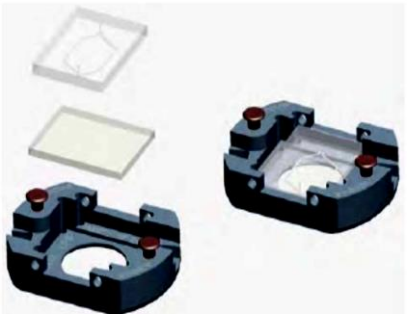

Figure 3.2: *Illustration of resealable chip interface and microfluidic devices [45].*

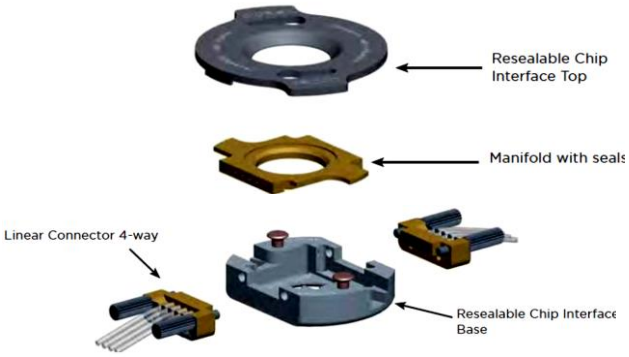

Figure 3.3: *Key components of the resealable chip interface [45].*

Afterward, silicon tubing connects the AF1 pressure pump (Elveflow) (Figure 3.4) with a reservoir containing the nutrient. Then, 0.5 mm interior diameter PTFE tubing connects the reservoir with the flow sensor (Elveflow) (Figure 3.5), in order to precisely control the flow rate, and finally with the flow perfusion culture system and the waste reservoir. Both the flow perfusion culture system and the waste reservoir are inside a 5% CO_2 incubator at 37 ^{o}C.

Figure 3.4: *Photography of the AF1 pressure pump [46].*

Figure 3.5: *Photography of the flow sensor [47].*

The thermal measurement principle by which the flow sensor controls the flow rate is a small heater that introduces a negligible amount of heat to the medium. Two temperature sensors, symmetrically positioned above and below the source of the heat, detect even the slightest temperature differences, thus providing the basic

information about the spread of the heat, which itself is directly related to the flow rate (Figure 3.6).

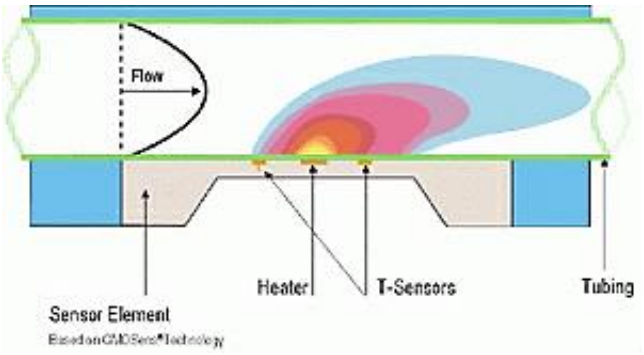

Figure 3.6: *Thermal measurement principle of the flow sensor* [48].

The images below show how the chips are loaded with cells (Figure 3.7) and then perfused with nutrient (Figure 3.8). The arrows in Figure 3.8 represent the direction of the flow.

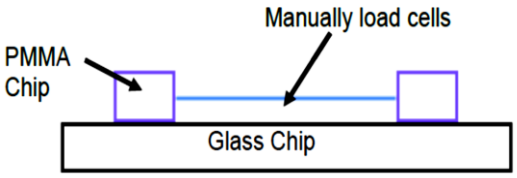

Figure 3.7: *Loading of cells.*

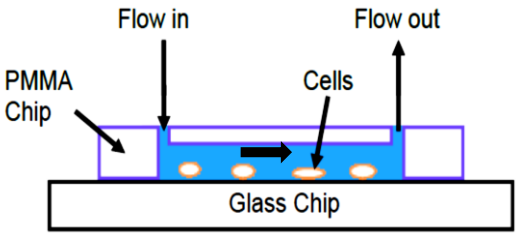

Figure 3.8: *Continuous perfusion of culture medium.*

3.2 Preparation of biomaterials

3.2.1 Gelatin films

A 2% w/v gelatin solution [gelatin (Sigma) was dissolved in water] was used for coating the glass base chip of the microfluidic system and dried for 2 hours before seeding the cells.

3.2.2 Collagen fiber networks

For the preparation of a 3 mg/ml collagen gel, a 6 mg/ml collagen stock solution [collagen (Sigma) was dissolved in 0.02 M acetic acid in water] was mixed with 10x

phosphate buffer saline (PBS) (Sigma) and water, followed by neutralization with NaOH 0.5 M. Then, the 3 mg/ml collagen solution was used for the chip coating. Gelation was performed by incubating the collagen solution for 48 hours at 4 °C for the formation of thick fibers [30, 49]. Thereafter, collagen gel dried for 3 hours, washed with water and 1x PBS (Sigma) and was completely immersed with culture medium overnight in a 5% CO_2 incubator at 37 °C before seeding the cells.

3.3 Rheological measurements of collagen gels

An Anton Paar (MCR 501) stress controlled rheometer was used for all measurements. In order to conduct rheological measurements with homogenous strain field and to avoid slippage, it was decided that the serrated cone and plate geometry (cone angle = 3.22°, diameter = 25 mm) was the most appropriate. A homemade solvent trap was used in all experiments completely sealing the sample from outside to create a closed saturated atmosphere and minimize evaporation. The measurements were performed at three different temperatures of 4 °C, 12 °C and 37 °C following a well-defined experimental protocol to ensure reproducibility of measurements. The measurements were conducted at (i) 4 °C, as this is the temperature of preparation of the collagen gels, (ii) 37 °C, as this is the physiological temperature in which cells are cultured in the incubator, and (iii) 12 °C as a selected intermediate temperature. More specifically, before dynamic frequency sweep tests we performed a shear induced rejuvenation. The rejuvenation consisted of a large amplitude oscillatory shear experiment, typically 1000% - 1% dynamic strain sweep at 1 rad/s, followed by setting stress at zero and waiting for 50 s. In fact, we rejuvenated our samples in order to destroy (erase) any structural memories that the system could have due to loading or preparation. In dynamic frequency sweep tests, we kept the strain constant in the linear regime and we measured G' and G'' as a function of frequency while in the dynamic strain sweep tests we measured G' and G'' as a function of strain at a constant frequency of 1 rad/s.

3.4 Cells and culture

MC3T3-E1 pre-osteoblastic cells were grown in cell culture flasks using culture medium [alpha-MEM (Sigma), supplemented with 10% FBS (Sigma), 2 mM glutamine (Sigma), 50 IU/mL penicillin (Sigma), and 50 g/mL streptomycin (Sigma)] in a 5% CO_2 incubator (Thermo Scientific or Heal Force) at 37 °C. Confluent cells were washed with 1x PBS (Sigma) and passaged after trypsinization [0.25% trypsin in 1 mM EDTA (Gibco)], seeded at 60–80% confluence and allowed to grow for 5 days before the next passage [50].

For cell differentiation experiments, cells were cultured in osteogenic medium [culture medium supplemented with 50 μg/mL ascorbic acid (Sigma) and 10 mM β-glycerophosphate (Sigma)] which initiates a development process that direct cells into an osteoblastic differentiation pathway [51, 52]. It has been shown [53, 54] that β-glycerophosphate favors mineralization by increasing the ability of phosphate ions, while ascorbic acid has a role in reducing the ion prosthetic group of hydroxylase enzymes responsible for collagen biosynthesis. Exposure to ascorbic acid and β-glycerophosphate stimulates procollagen hydroxylation, processing and fibril assembly followed by the induction of specific genes associated with the osteoblast phenotype, such as alkaline phosphatase, osteopontin and osteocalcin [55, 56].

3.5 Viscosity of the osteogenic medium

We measured the viscosity of the osteogenic medium, with the use of a microviscometer (Lovis 2000), and we found that it is 0.01078 $gcm^{-1}s^{-1}$.

The Lovis 2000 is a rolling ball viscometer (Figure 3.9) which measures the rolling time of a ball through transparent and opaque liquids according to Höppler's principle: A ball rolls through a liquid-filled capillary that is inclined at a defined angle. Three inductive sensors measure the ball's rolling time through transparent and opaque liquids between defined marks. The liquid's viscosity is directly proportional to the rolling time, as shown in the following equation:

$$\eta = K \cdot (\rho_b - \rho_s) \cdot t \qquad \textit{(equation 3.1)}$$

where η is shear viscosity, K is a constant, ρ_b is ball density, ρ_s is sample density and t is rolling time.

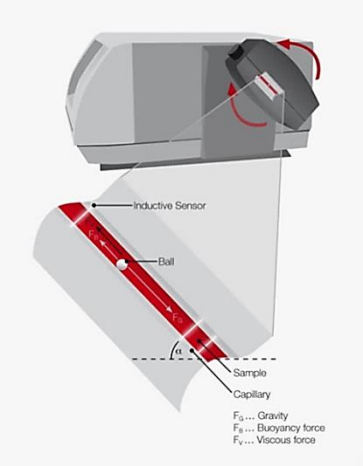

Figure 3.9: *Illustration of the Lovis 2000 microviscometer* [57].

3.6 Static and dynamic cell cultures

At first, in order to enhance initial cell adhesion, as well as, proliferation and differentiation of pre-osteoblastic cells, the inner surface of the flow perfusion culture system (glass base chip) was coated with gelatin film and collagen fiber networks. Then $8x10^4$ cells/cm^2 were cultured on the glass base chip, which was coated either with gelatin film or collagen fibers and kept at rest overnight in a 5% CO_2 incubator at 37 ^oC. The next day, the perfusion of the culture was started and completed inside the CO_2 incubator. The osteogenic medium in the reservoir was changed every 3 days. Flow rates of 30, 50, 75, 100 μl/min were used when the gelatin film was used as a substrate while 30 and 50 μl/min when collagen fibers were used.

The flow rates that we used, and consequently the speed, are similar to those of the small arteries in the bloodstream (arterioles, capillaries, and venules). Tables 3.1 and 3.2 show the flow rates and speed in the blood circulation and in the microfluidic system, respectively.

Blood circulation				
Vessel	**υ (m/s)**	**d (mm)**	**Q (l/min)**	**Q (μl/min)**
Aorta	0.4	25	11.8	$11.8 \cdot 10^6$
Arteries	0.45	4	0.3	300000
Arterioles	0.05	0.05	$5.9 \cdot 10^{-6}$	5.9
Capillaries	0.001	0.008	$3 \cdot 10^{-9}$	$3 \cdot 10^{-3}$
Venules	0.002	0.02	$3.8 \cdot 10^{-8}$	0.038
Veins	0.1	5	0.12	120000
Vena cava	0.38	30	16.1	$16.1 \cdot 10^6$
Flow rate = $\frac{\pi \cdot (\text{pipe diameter})^2 \cdot \text{velocity}}{4}$				

Table 3.1: *Values for velocity υ (m/s), diameter d (mm) and flow rate Q (l/min and μl/min) of the vessels in the blood circulation* [58].

Our microfluidic system		
Q (μl/min)	**d (mm)**	**υ (m/s)**
30	0.5	0.0026
50	0.5	0.0042
75	0.5	0.0064
100	0.5	0.0085
Velocity = $\frac{4 \cdot \text{flow rate}}{\pi \cdot (\text{pipe diameter})^2}$		

Table 3.2: *Values for flow rate Q (μl/min), diameter d (mm) and velocity υ (m/s) in the microfluidic system.*

The shear stress, σ, exerted on the cell layer is predicted by the equation [59]:

$$\sigma = (6\eta Q) / (bh^2)$$

where η is the viscosity of the osteogenic medium (η=0.01078 $gcm^{-1}s^{-1}$), Q is the volumetric flow rate, b is the width of the PMMA chip with PDMS gasket for flowing fluids across the cells and substrates (b=11 mm) and h is the height of gasket (h=100 μm). Table 3.3 shows the flow rates and the shear stresses in the microfluidic system.

Our microfluidic system	
Q (μl/min)	**σ (dynes/cm²)**
30	0.3
50	0.5
75	0.7
100	1

Table 3.3: *Values for flow rate Q (μl/min) and shear stress σ (dynes/cm²) in the microfluidic system.*

For comparative purposes, $8x10^4$ cells/cm^2 were also cultured under static conditions, both in the interior of the flow perfusion culture system and in conventional static cultures, which were coated with gelatin film or collagen fibers. Finally, the osteogenic medium was changed every 3 days.

3.7 Osteogenic markers response of MC3T3-E1 cells

We determined the alkaline phosphatase (ALP) activity, and the total soluble collagen contents in the culture medium using an enzymatic activity assay and a modified Sirius red assay [60], respectively, which are described in detail below.

3.7.1 Alkaline phosphatase (ALP) activity

The alkaline phosphatase (ALP) catalyzes the hydrolysis of the colorless organic phosphate ester substrate, p-nitrophenylphosphate, to the yellow colored product p-nitrophenol and phosphate. The rate of color change corresponds to the amount of enzyme present in solution and is measured spectrophotometrically at 405 nm.

More specifically, the cell – biomaterial constructs were removed from the inner surface of the flow perfusion culture system or from the static culture after trypsinization on day 7. Then, they were placed in 1.5 mL eppendorf tubes,

centrifuged at 4000 rpm for 15 minutes and washed with 1 mL 1x PBS. Afterward, 100 μL lysis buffer [0.1% Triton X-100 (Sigma) in Tris/HCl pH 10] was added in each tube and they were incubated overnight in a freezer at -80 ^{o}C. The next day the cell – biomaterial constructs were thawed. For the assay, 96-well plates were used. In each well 95 μL lysate or 95 μL lysis buffer (as blank), 5 μL Tris/HCl pH 10 and 100 μL of 2 mg/mL p-nitrophenylphosphate (pNNP) substrate [2 mg/mL pNNP substrate (Sigma) solution in 50 mM Tris/HCl pH 10] were added and the plate was incubated for 60 minutes at 37 ^{o}C. Finally, the absorbance was measured in a spectrophotometer (Molecular Devices SpectraMax M2 or SYNERGY|HTX) at a wavelength of 405 nm and the alkaline phosphatase activity was determined by means of a calibration curve.

The total protein concentration was determined using the Bradford reagent (Sigma) according to the manufacturer's instructions [61]. The Bradford protein assay is a simple procedure for the determination of total protein concentrations in solutions that depends upon the change in absorbance based on the proportional binding of the dye Coomasie Blue G-250 to proteins. The Coomasie Blue G-250 dye appears to bind most readily to arginyl and lysyl residues of proteins, causing a visible color change which is measured spectrophotometrically at 595 nm [61].

Specifically, 5 μL lysate or 5 μL lysis buffer (as blank), 15 μL Tris/HCl pH 10 and 200 μL Coomasie Blue G-250 were added in each well of the 96-well plate and were incubated for 5 minutes at room temperature. The absorbance was then measured in a spectrophotometer at a wavelength of 595 nm and the total protein concentration was determined by means of a calibration curve.

3.7.2 Collagen production

A modified Sirius red assay [60] was used in order to stain the collagen produced in the extracellular matrix. Sirius red F3B is an elongated molecule containing six sulphonic acid groups and its length is approximately 46 Å. As collagen is a basic protein it is probable that the sulphonic groups of the dye may interact at low pH with the amino groups of lysine and hydroxylysine and the guanidine groups of arginine [62]. After binding of the dye, the collagen-dye complex precipitates, resulting in a colored pellet and this color can be released in an alkaline solution. The rate of color change corresponds to the amount of protein present in solution and is measured spectrophotometrically at 530 nm.

$8x10^4$ cells/cm^2 were cultured both under static and dynamic conditions (flow rates of 30 and 50 μl/min), in the interior of the flow perfusion culture system, as well as, in conventional static cultures, which were coated with gelatin film. The supernatants were collected the fourth and the seventh day for the determination of collagen produced in the extracellular matrix. More specifically, 75 μL of water were added into 25 μL of sample (supernatant) or blank (plain culture medium) in duplicate into 2

mL eppendorf tubes. Then, 1 mL of the dye solution [0.1 gr Sirius red F3B (Sigma) dissolved in 100 mL acetic acid 0.5 M] was added and the samples were incubated at room temperature for 30 minutes. Afterward, the samples were centrifuged at 15000 G for 15 minutes to pellet the collagen-dye complex. The supernatant was drained off, without disturbing the pellet, by inverting the tubes onto an absorbent paper. 0.5 mL of 0.1 M HCl was then added to each tube so as to remove the unbound dye and was vortexed. The samples were centrifuged at 15000 G for 15 minutes to pellet the collagen and the supernatant was drained off well. 0.5 mL of 0.5 M NaOH was added to each tube and was vortexed vigorously so as to release the bound dye. Finally, 200 μL of the solution were transferred to a 96-well plate. The absorbance was measured in a spectrophotometer at a wavelength of 530 nm and the collagen was determined by means of a calibration curve.

3.8 Morphology of MC3T3-E1 cells

3.8.1 Optical Microscopy

MC3T3-E1 cells were visualized the first, fourth and seventh day by optical microscopy by means of a Zeiss Axiovert 200 microscope. Images were taken by a ProgRes® CFscan Jenoptik camera (Jena, Germany) using the ProgRes® CapturePro 2.0 software and objective lens for 10 fold magnification.

3.8.2 Scanning Electron Microscopy (SEM)

$2x10^4$ MC3T3-E1 cells in culture medium were seeded on collagen fiber networks and placed in the CO_2 incubator at 37 ^oC for one day. Then, the samples were removed from the incubator, washed twice with 0.1 M sodium cacodylate buffer (SCB) and fixed with 2% glutaraldehyde (GDA) and 2% paraformaldehyde (PFA) in 0.1 M SCB for 30 minutes. Thereafter, they were washed twice with 0.1 M SCB and dehydrated in increasing concentrations (from 30-100%) of ethanol. Finally, they were dried in a critical point drier (Baltec CPD 030), sputter-coated with a 20-nm thick layer of gold (Baltec SCD 050) and observed under a scanning electron microscope (JEOL JSM-6390 LV) at an accelerating voltage of 15 kV [63].

3.9 Observation of collagen fibrous network in SEM

The collagen fibrous material samples were dried for 3 hours, sputter-coated with a 20-nm thick layer of gold (Baltec SCD 050) and observed by placing them in the sample holder in perpendicular position under a scanning electron microscope (JEOL

JSM-6390 LV) at an accelerating voltage of 15 kV. The images captured show cross sections of the collagen fibrous material samples on the glass substrates.

4. Results and Discussion

4.1 Characterization of a fibrous collagen substrate for cells

4.1.1 SEM images of collagen fiber networks

Scanning Electron Microscopy (SEM) was used to picture the morphology of the collagen fiber networks (Figure 4.1), as well as, to visualize the cell – biomaterial constructs in order to assess cell morphology (Figure 4.2). More specifically, Figure 4.1 depicts the formation of a network with thick fibers, after incubation at 4 ^{o}C for 48 hours, at 3000x magnification. Figure 4.2 illustrates the cell – biomaterial interaction, after one day of culture, at 3000x magnification. On the first day, most cells exhibited a branched shape and flattened morphology with long cellular extensions that signal good adhesion and growth of the cells on the collagen fibers [63].

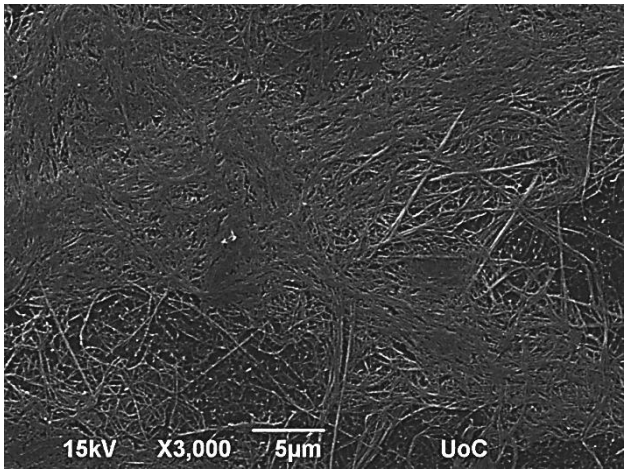

Figure 4.1: *Scanning electron microscopy image showing the morphology of collagen fiber networks.*

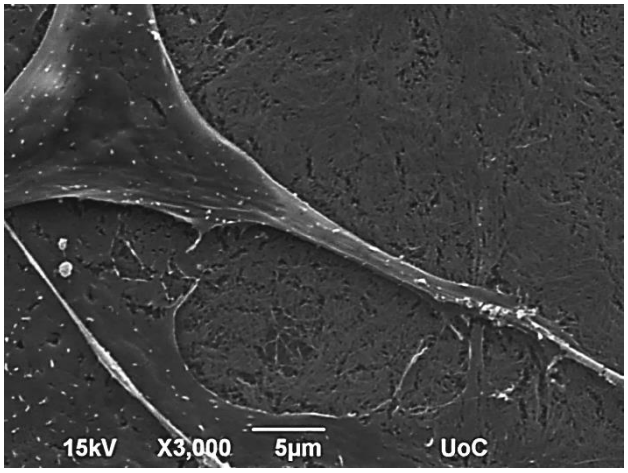

Figure 4.2: *Scanning electron microscopy image showing the morphology of MC3T3-E1 cells after 1 day of culture on collagen fiber networks.*

The thickness of the collagen fiber networks was determined by SEM after the creation of a sample cross-section analysis and was found to be around 700 nm. Figure 4.3 depicts a cross-section image of the collagen fiber networks obtained by scanning electron microscopy.

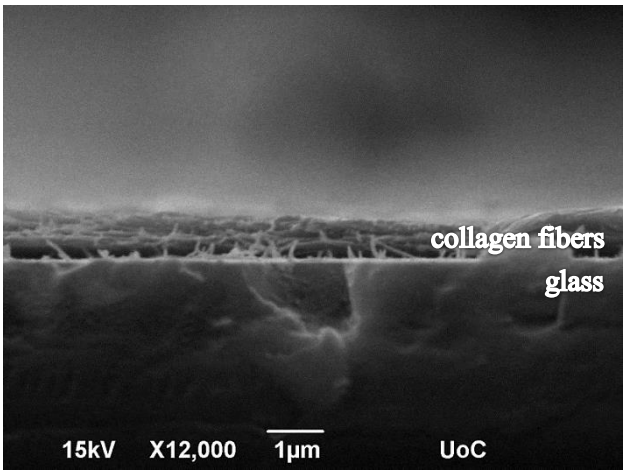

Figure 4.3: *SEM image of a sample cross-section showing the collagen fiber networks prepared on a glass substrate.*

4.1.2 Rheological investigation of collagen hydrogels

4.1.2.1 Linear Rheology

Generally, dynamic frequency sweep tests were performed in order to determine the elastic (G') and viscous (G'') moduli. In Figure 4.4 we show the linear viscoelastic data of a 3 mg/ml collagen gel prepared at 4 ^{o}C, at three different temperatures of 4 ^{o}C, 12 ^{o}C and 37 ^{o}C. We chose these temperatures because at 4 ^{o}C is the temperature where we prepared the collagen gel, 37 ^{o}C is the temperature of the incubator where cells are cultured and 12 ^{o}C is an intermediate temperature. The dynamic frequency sweeps were performed in the linear regime with a strain of 0.5% determined by dynamic strain sweeps performed at a frequency of 1 rad/s. The spectra are characterized by a storage modulus (G'), which rises up in the frequency range investigated in the study, and a loss modulus (G'') that is an order of magnitude lower than the corresponding storage modulus. Moreover, the values of G' were larger than G'' for all temperatures over the applied frequencies, implying that the gel exhibited more solid-like than liquid-like viscoelastic behavior. Finally, the rheological results indicated that G' and G'' of the collagen gel increased with lower temperature.
The larger G' values of the collagen gel at the temperature of 4 ^{o}C were attributed to the formation of thicker fibers caused by the longer nucleation phase. It has been shown [49] that the lag (nucleation) phase, in which the soluble collagen particles accrete to perform nuclei (activation) centers, predominates over growth (exponential)

phase and the size of fibrils is determined during this lag period. Lower temperature provides longer lag phase which results in thickening of the collagen fiber structure.

The increase of the storage modulus with frequency is due to the fact that the collagen fibrils were able to keep entangled like the pseudo-cross-link as a result of the lack of enough time to loosen it [64]. At lower shear frequencies, however, the entangled collagen fibrils could slide freely each other resulting in a lower G' value.

The G' value represents the capability of resilience storage and deformation resistance. A higher G' value corresponds to a stiffer gel. When cells spread on collagen gel, contractile forces are spontaneously produced and applied to the collagen matrix. If the collagen gel possesses a larger elasticity, it could bear a greater contractile force to avoid the deformation and provide a larger mechanical support for the need of the cell growth [65]. Indeed, cells feel the stiffness of the gel and respond by remodeling the cytoskeleton and modulating intracellular signaling pathways for proliferation and differentiation [11-18].

To conclude, the elasticity of the collagen gel prepared at 4 ^{o}C and measured at 37 ^{o}C was lower than those which measured at 4 ^{o}C. However, this elasticity was adequate to provide mechanical support to the cells and enhance the proliferation and differentiation, as presented below.

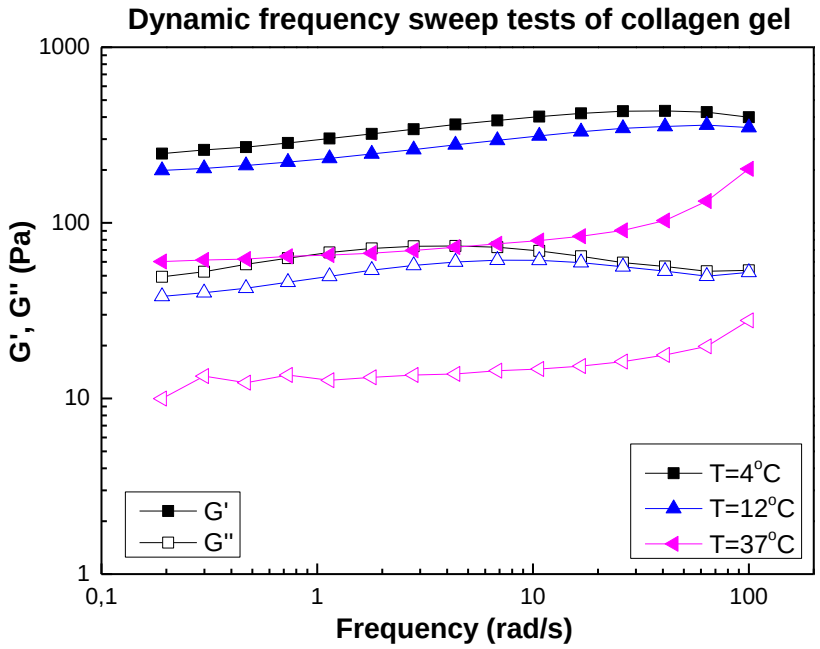

Figure 4.4: *Dynamic frequency sweep tests of a 3 mg/ml collagen gel at three different temperatures of 4 ^{o}C, 12 ^{o}C, and 37 ^{o}C. G' is represented by solid symbols and G'' by open ones.*

4.1.2.2 Non-Linear Rheology

In Figure 4.5 we present the dynamic strain sweep measurements of a 3 mg/ml collagen gel prepared at 4 ^{o}C at three different temperatures of 4 ^{o}C, 12 ^{o}C, and 37 ^{o}C. The measurements were conducted at a frequency of 1 rad/s and were plotted as a function of strain. The linear regime, where the solid-like behavior of the collagen gel is demonstrated is extended to be about 0.2 – 2% strain amplitude. Above this value, shear thinning sets in with G' decreasing and G'' increasing with strain amplitude. At about 17 – 90% strain, G'' crosses over G' which is a characteristic of transition from viscoelastic solid to liquid-like behavior and thus provides a measurement of the yield strain at G'=G'', as indicated in the Figure 4.5 (see vertical arrow).

Interestingly, for all three temperature conditions, we observe a pronounced drop of the G' and G'' values with increasing strain. Moreover, it is observed that the yield strain, $\gamma_{y,}$ increases with higher temperatures. Such a behavior is attributed to differences in network organization. As mentioned before, collagen's microstructure is dependent on temperature. A collagen gel constructed at temperatures below 37 ^{o}C is expected to have thicker fibers composed of individual fibrils which are straighter and longer than those at 37 ^{o}C [66]. As a result, the alignment of the fibrils can be achieved at lower strains resulting in smaller values of yield strain.

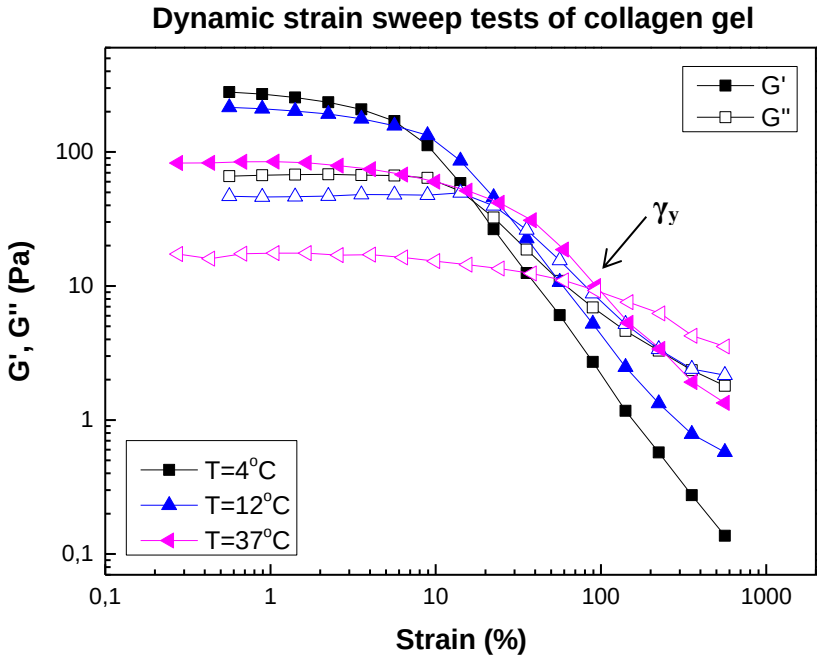

Figure 4.5: *Dynamic strain sweep tests of a 3 mg/ml collagen gel at three different temperatures of 4 ^{o}C, 12 ^{o}C, and 37 ^{o}C. G' is represented by solid symbols and G'' by open ones.*

4.2 Morphology and orientation of pre-osteoblastic cells under various conditions

4.2.1 Cell morphology in static cultures on gelatin and tissue culture treated polystyrene as control surfaces

In these pictures we show the cell morphology in static cultures for two different time points (4 days and 7 days) and three different surfaces [tissue culture treated polystyrene (PS), 2% w/v gelatin on glass and 2% w/v gelatin on microdevice glass] in order to control the cell adhesion and substrate. We notice that the cells attach well exhibiting a spindle-like elongated shape and filopodia [34, 67, 68] and proliferated well in all surfaces (Figure 4.6).

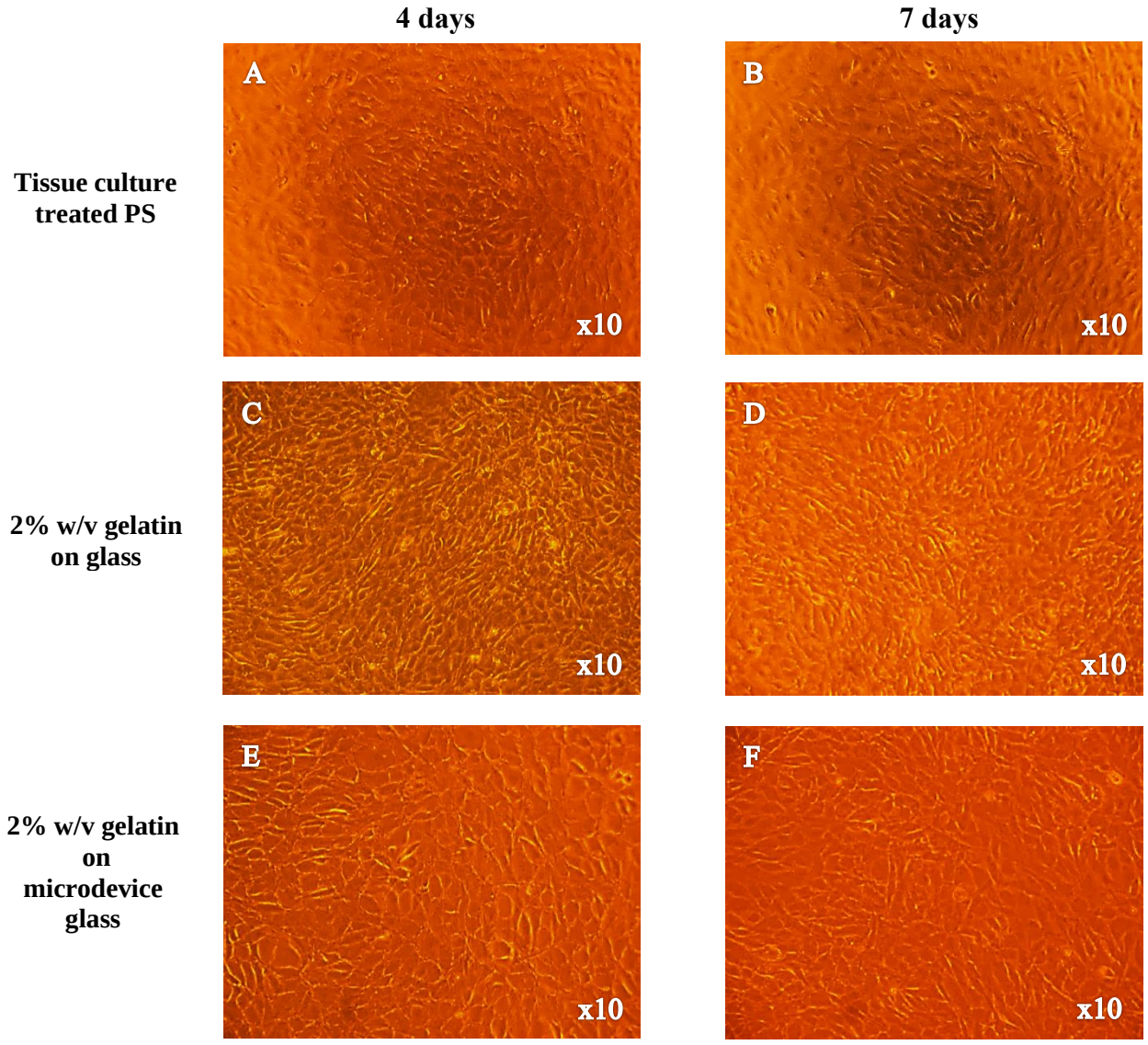

Figure 4.6: *Morphology of MC3T3-E1 cells in static cultures after 4 days (A, C, E) and 7 days (B, D, F) in different surfaces, tissue culture treated PS (A, B), 2% w/v gelatin on glass (C, D) and 2% w/v gelatin on microdevice glass (E, F) using optical microscopy.*

4.2.2 Cell morphology in static cultures on a fibrous collagen network

Similar to gelatin substrate, the pre-osteoblastic cells adhere strongly and proliferate, when using collagen fiber networks as a substrate, both on the glass and on the microdevice glass, as observed in Figure 4.7.

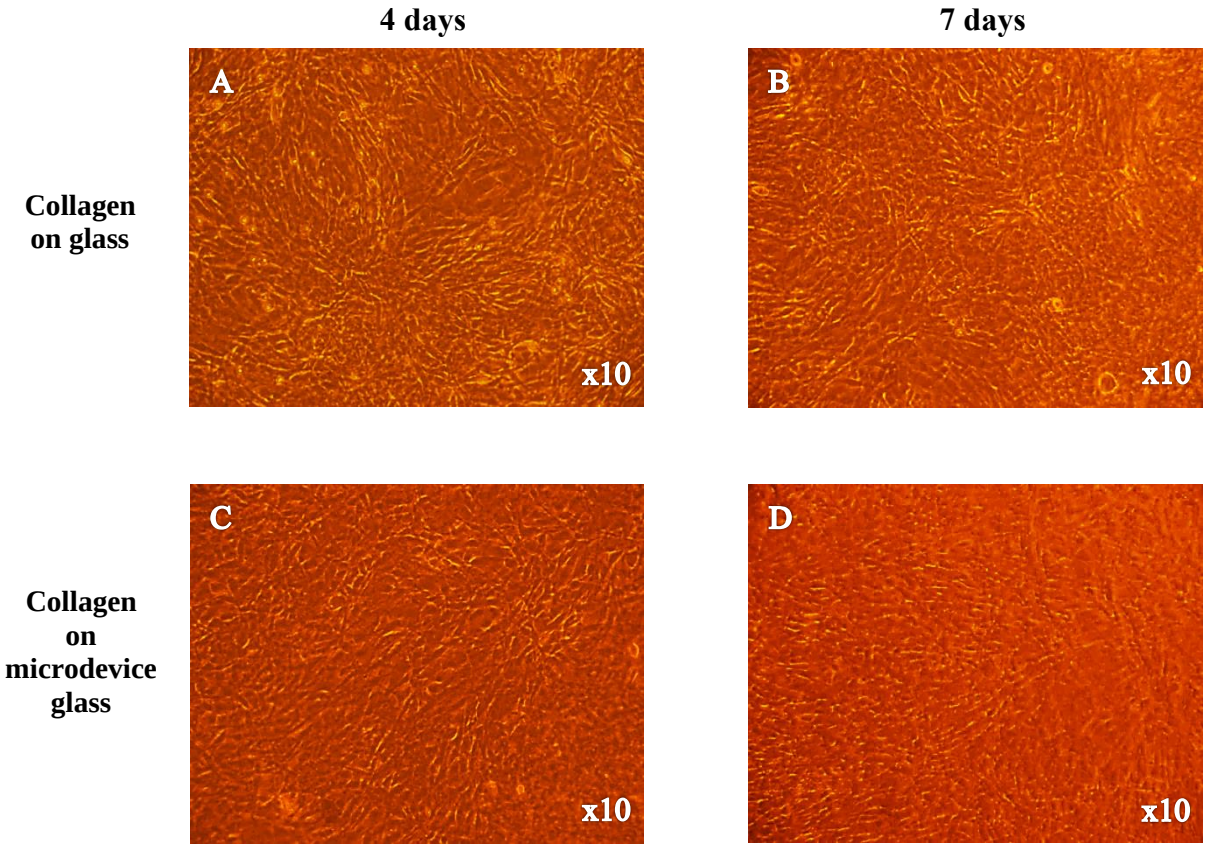

Figure 4.7: *Morphology of MC3T3-E1 cells in static cultures with the use of collagen fiber networks as a substrate after 4 days (A, C) and 7 days (B, D) on glass (A, B) and on microdevice glass (C, D) using optical microscopy.*

4.2.3 Dynamic cell cultures on gelatin and glass in the flow perfusion culture system

Figure 4.8 illustrates the cell morphology in dynamic cultures at different time points (day 1 without flow, day 3 after flow and day 6 after flow) under flow rates of 30 and 50 μl/min. Under flow conditions, the pre-osteoblastic cells after three days of perfusion appear to be oriented along the direction of flow, whereas cells depict a random orientation under static conditions. The arrows in Figure 4.8 represent the direction of the flow.

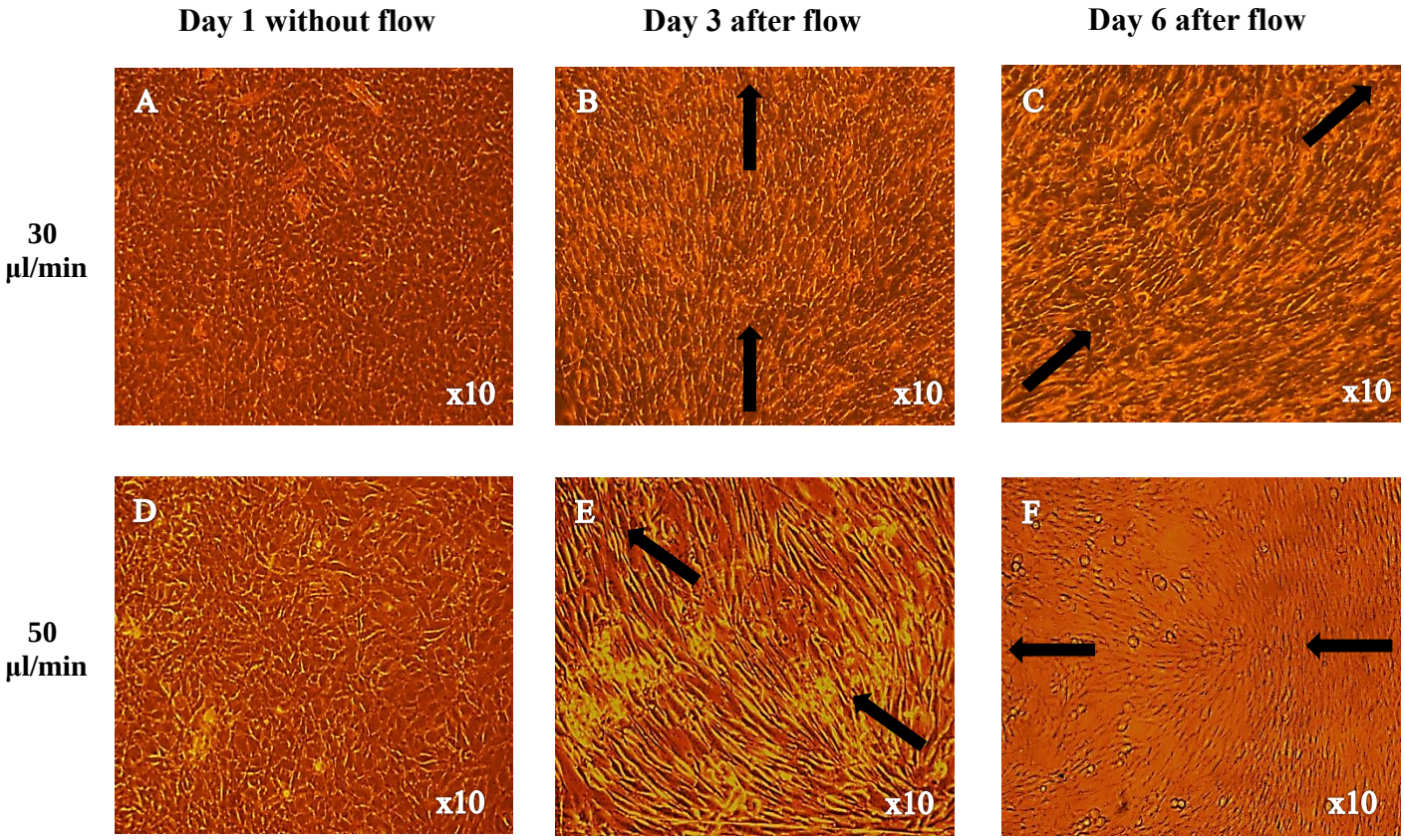

Figure 4.8: *Morphology of MC3T3-E1 cells inside the flow perfusion culture system under static conditions (A, D), and under flow conditions applying 30 (B, C), and 50 µl/min (E, F) using optical microscopy.*

4.2.4 Dynamic cell cultures on a fibrous collagen network in the flow perfusion culture system

Similarly, an orientation of osteoblastic cells was noticed after three days of perfusion when using collagen fiber networks as a substrate, under flow rates of 30 and 50 µl/min (Figure 4.9). The arrows in Figure 4.9 show the direction of the flow.

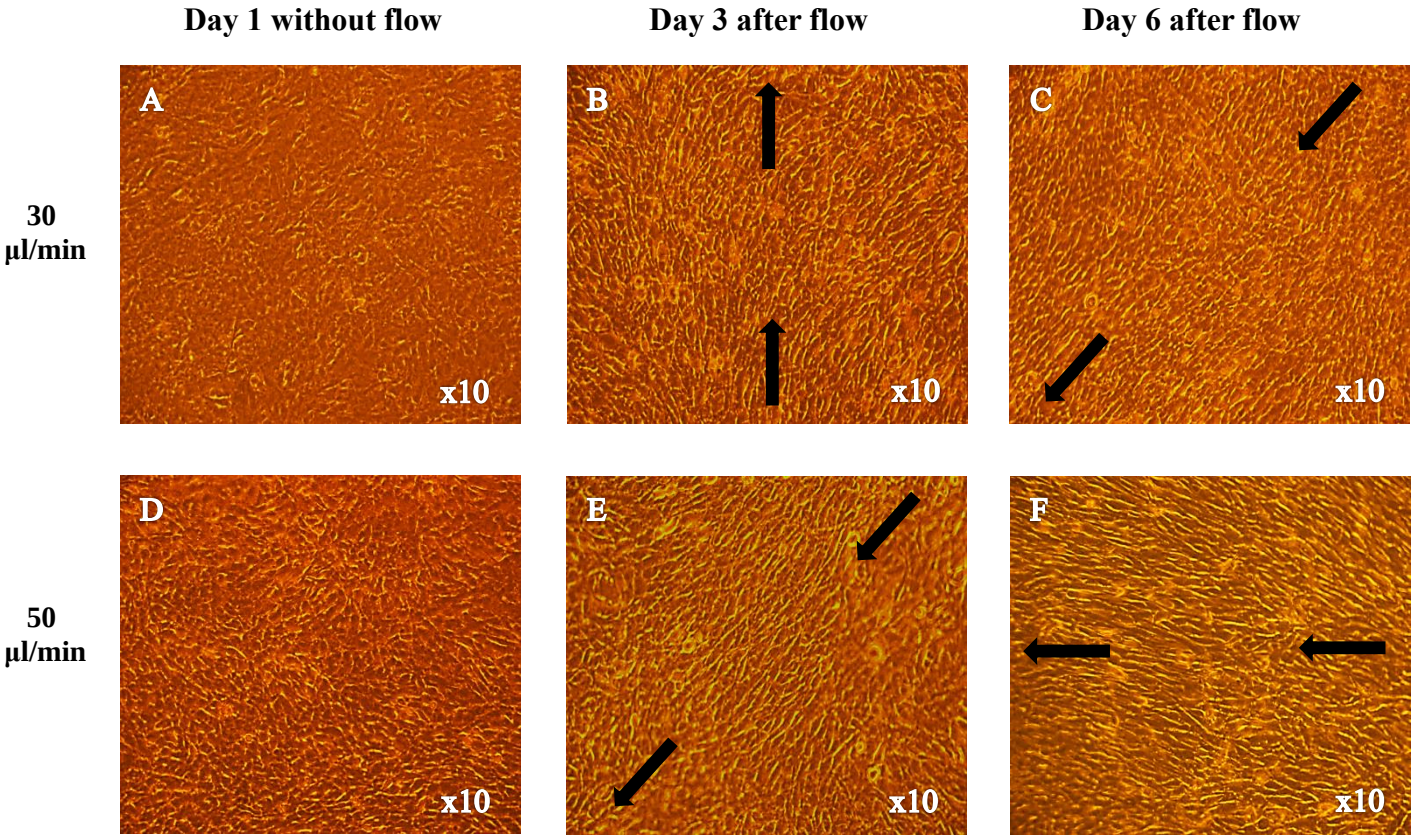

Figure 4.9: *Morphology of MC3T3-E1 cells inside the flow perfusion culture system with the use of collagen fiber networks as a substrate under static conditions (A, D), and under flow conditions applying 30 (B, C), and 50 µl/min (E, F) using optical microscopy.*

Bone remodeling occurs due to the fact that bone cells respond to mechanical stimulations. One of the main mechanical stimulations on bone cells, *in vivo*, is the interstitial fluid flow stress in the lacunae-canaliculi network [69]. *In vivo*, the magnitude of the fluid flow stress in bone tissue is estimated to be between 8 and 30 dynes/cm^2 [70, 71]. It has been shown [72, 73] that osteoblasts have been used to investigate the morphological and functional responses to fluid shear stresses *in vitro*. The values of the shear forces reported to be stimulatory for pre-osteoblastic cells cultured in two-dimensional flow chambers for short periods are higher than 2 dynes/cm^2 [74].

In bone cells, the cytoskeleton is considered to be the major factor that influences the cellular morphology and biomechanical response [75]. Cellular morphology determines cellular function and is related to the organization of cellular cytoskeletal components.

The cytoskeleton is a fundamental structural unit composed of a network of microfilaments and microtubules. When the cytoskeleton is elongated, more docking and activation sites for focal adhesions are created, which act as mechanical linkages to the extracellular matrix. Mechanical stimulation causes also changes in cytoskeletal organization producing different cellular responses.

In our study, the approximate fluid shear forces experienced by the cells were calculated to be in the range of 0.3 - 0.5 dynes/cm^2. Osteoblasts were able to respond to these fluid shear forces both morphologically, as it is shown in the figures above, and functionally, as presented in the next chapters.

4.3 Proliferation of pre-osteoblastic cells under various conditions

The results of the determination of total protein concentration on the seventh day, when used collagen fiber networks as a substrate, are depicted in Figure 4.10. A significant difference in the proliferative cell behavior is observed between the dynamic condition with the flow rate of 50 μl/min and the static conditions ($p<0.05$). No significant differences were observed between static cultures and dynamic culture with the flow rate of 30 μl/min.

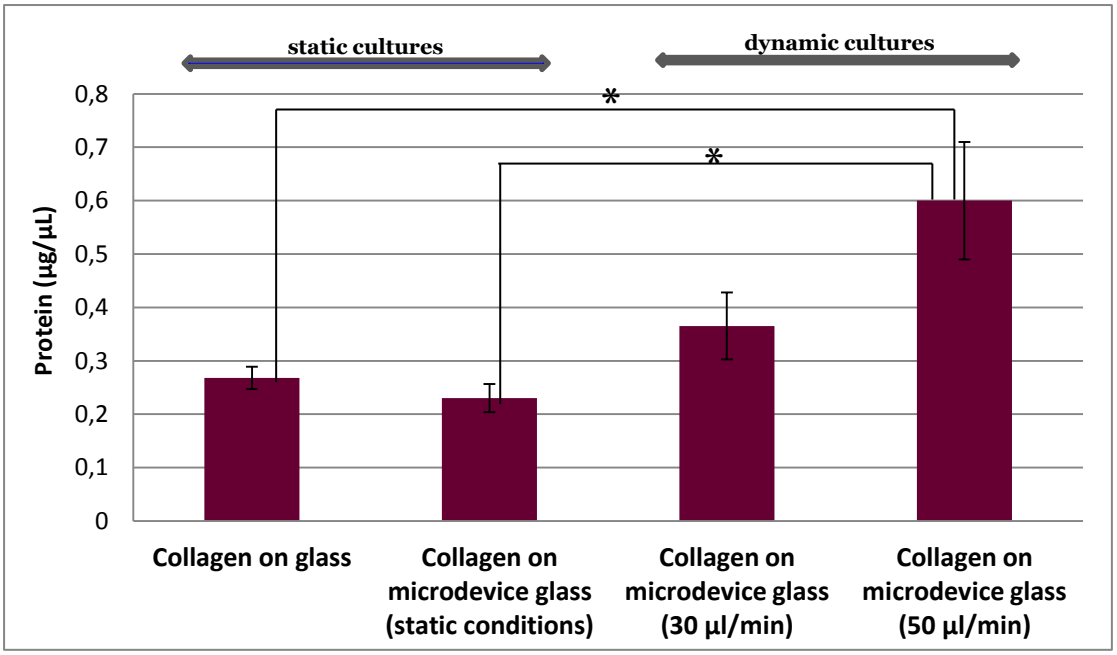

Figure 4.10: *Protein concentration of MC3T3-E1 cells after 7 days of culture under static conditions (glass and microdevice glass) and under flow conditions (flow rates of 30 and 50 μl/min) with the use of collagen fiber networks as a substrate, in the presence of osteogenic medium.*

The determination of protein concentration showed a significant increase in the proliferation of cells on collagen fibers subjected to a flow rate of 50 μl/min compared to static conditions. This is in agreement with reports from other research groups [76 - 79], showing that the use of dynamic cultures leads to increased cell proliferation. A possible explanation could be the improved supply of nutrients and mass transport of oxygen inside the collagen fibers. Indeed, in static cultures there are mass transport limitations to the interior of the collagen fibers which are removed under flow conditions. Furthermore, the continuous flow could enhance the effective waste removal of cell metabolic products from the interior of the fibers network. The stimulatory effects of fluid flow on the proliferation of pre-osteoblastic cells seeded on collagen fibers could also be attributed to the fluid shear forces cells are experiencing and the enhanced chemotransport provided by the continuous perfusion of the medium. Conclusively, the collagen fibers are able to support greater cell growth under flow conditions as evidenced by the higher concentration of protein compared to static conditions.

4.4 Osteogenic response of pre-osteoblastic cells

4.4.1 Alkaline phosphatase (ALP) activity in static and dynamic cultures

ALP is known to be an early marker for the osteoblast phenotype, being up-regulated at the onset of differentiation and subsequently decreasing as differentiation progresses [77]. The ALP activity of pre-osteoblastic cells is an indicator of their commitment towards the osteoblastic lineage [80].

The ALP activity was determined on the seventh day of culture and normalized with the total protein concentration as shown in Figure 4.11. The first two bars indicate the static cultures (tissue culture treated PS and 2% w/v gelatin on glass) while the last four the dynamic cultures, with the use of gelatin film as a substrate, under flow rates of 30, 50, 75 and 100 μl/min. We observed that the normalized ALP activity was similar between conventional static cultures and dynamic cultures, except the flow rate of 100 μl/min, which was lower. An explanation for this could be the cell detachment under this high flow, which caused a systematic decrease in cell number with increasing duration of flow.

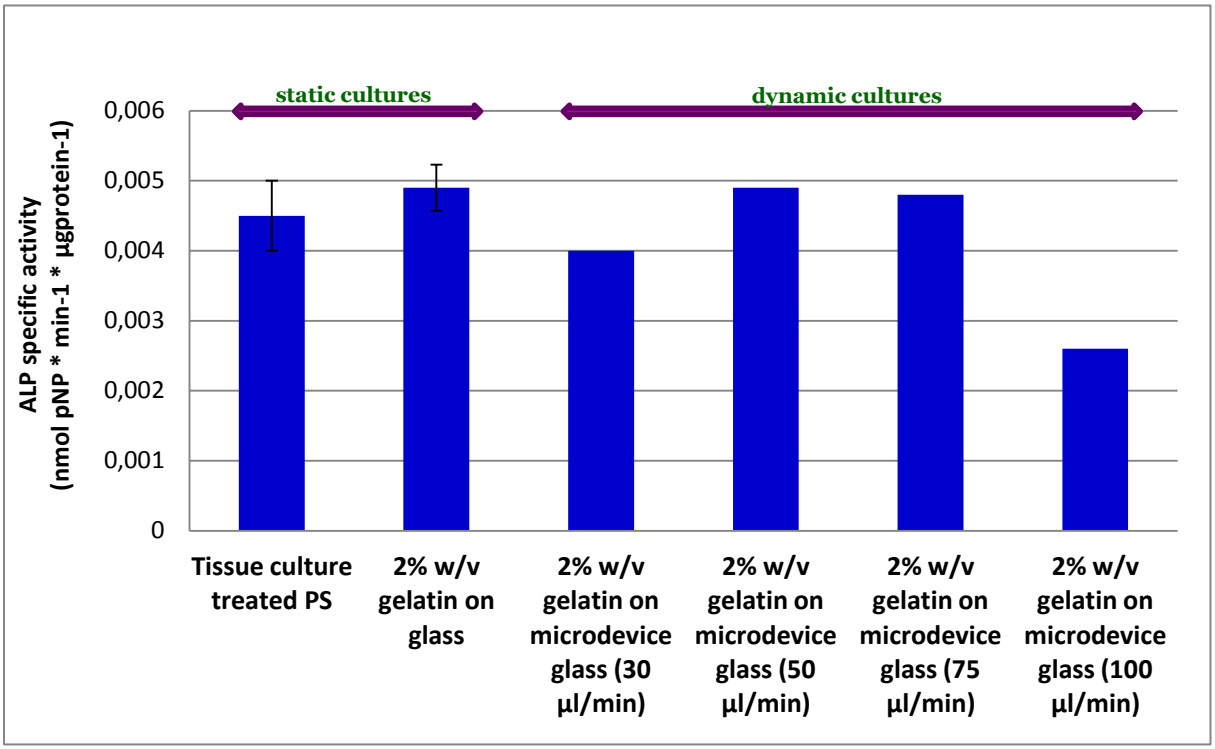

Figure 4.11: *Normalized ALP activity of MC3T3-E1 cells after 7 days of culture under static conditions (tissue culture treated PS and 2% w/v gelatin on glass) and under flow conditions (flow rates of 30, 50, 75 and 100 µl/min) with the use of gelatin film as a substrate, in the presence of osteogenic medium.*

Interestingly, when we used collagen fiber networks as a substrate, the normalized ALP activity on the seventh day was significantly higher ($p<0.05$) in dynamic culture with the flow rate of 30 µl/min compared to static culture (collagen on glass). No significant differences were observed between static conditions and dynamic condition with the flow rate of 50 µl/min (Figure 4.12).

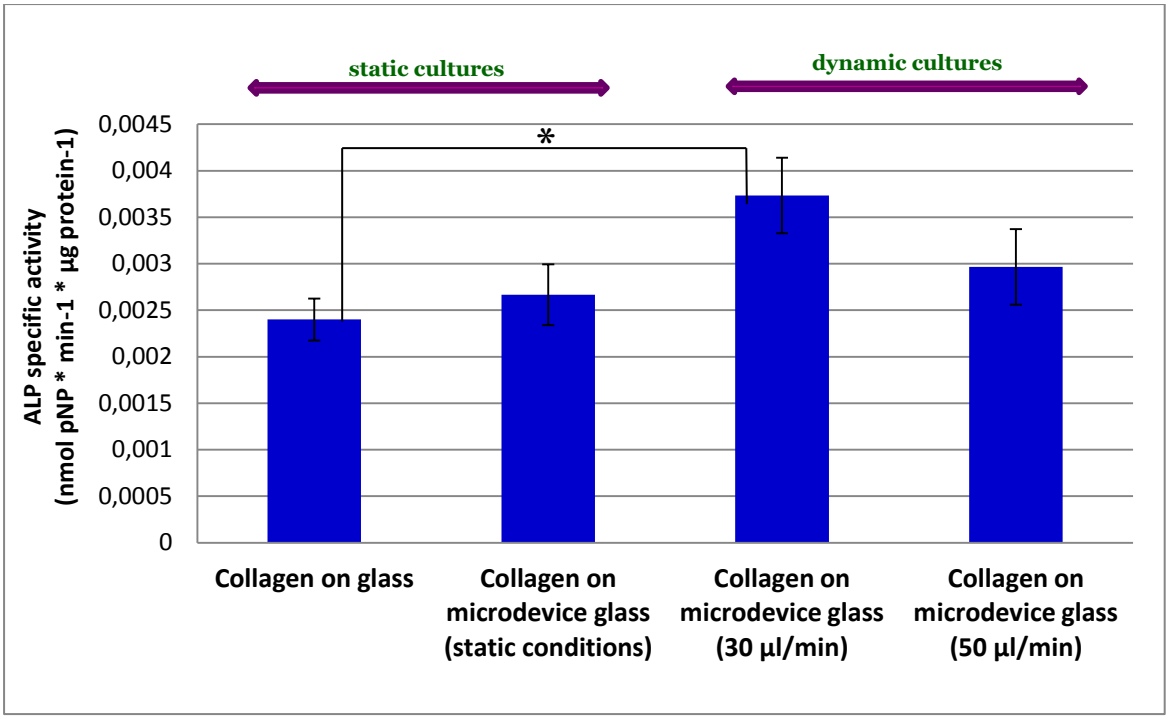

Figure 4.12: *Normalized ALP activity of MC3T3-E1 cells after 7 days of culture under static conditions (glass and microdevice glass) and under flow conditions (flow rates of 30 and 50 µl/min) with the use of collagen fiber networks as a substrate, in the presence of osteogenic medium.*

The temporal expression of cell growth and expression of the osteoblastic phenotype has three periods: i) A period of strong proliferation accompanied by the formation of extracellular collagenous matrix, ii) a matrix maturation phase featured with a decrease of proliferation and increase of ALP expression, and iii) a mineralization phase marked with a further decrease of proliferation, a decline of the ALP activity, and the formation of mineralized extracellular matrix [80].

We observed that the normalized ALP activity of cell – biomaterial constructs cultured under dynamic conditions with a flow rate of 30 µl/min, was significantly higher compared to static conditions in agreement with other studies [9, 76, 81]. The levels of the normalized ALP activity under the flow rate of 50 µl/min were similar to the static cultures. The fact that the normalized ALP activity under the flow rate of 50 µl/min was not higher than under static conditions may be explained due to the enhanced proliferation of the cells (as it is presented in chapter 4.3) as a dominating process against the differentiation during the experimental period of seven days.

It is not clear, if the enhanced proliferation and differentiation of pre-osteoblastic cells on the collagen fibers is solely due to the improved nutrient supply within the collagen fibers, or due to the stimulation of the seeded cells through their exposure to

fluid shear forces. Probably both events are involved in controlling cell proliferation and differentiation [76].

As mentioned before, the approximate fluid shear forces experienced by the cells were calculated to be in the range of 0.3 - 0.5 dynes/cm^2. The values of the shear forces reported to be stimulatory for pre-osteoblastic cells cultured in 2D flow chambers, for short period, were at least one order of magnitude higher, 2 - 20 dynes/cm^2 [74]. However, our results indicate that shear forces in the range of 0.3 - 0.5 dynes/cm^2 are adequate to enhance the proliferation and differentiation of pre-osteoblastic cells in long-term cultures.

4.4.2 Collagen production in static and dynamic cell cultures

Figure 4.13 illustrates the normalized levels of collagen (collagen / protein) produced in the extracellular matrix on the seventh day under static and dynamic conditions when gelatin film was used as a substrate. We observed that the collagen secreted by MC3T3-E1 cells under the flow rate of 30 μl/min was significantly higher compared to static conditions ($p<0.01$), with a remarkably significant increase when applying the flow rate of 50 μl/min ($p<0.01$).

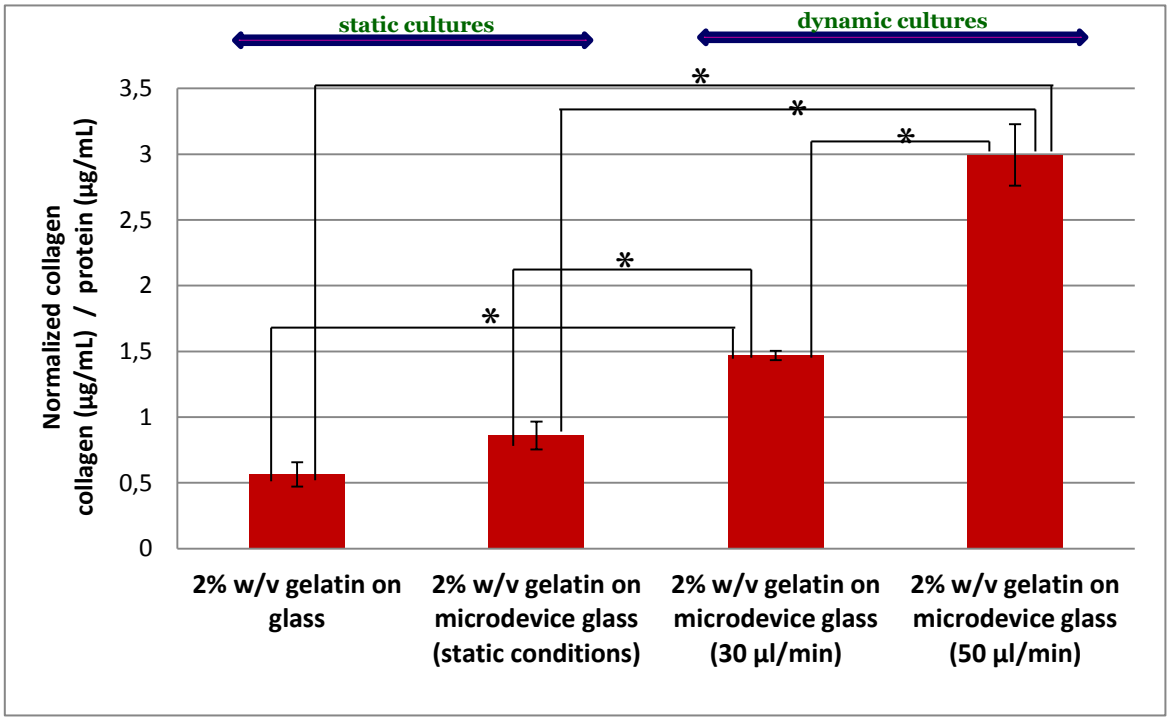

Figure 4.13: *Normalized levels of collagen secreted by MC3T3-E1 cells after 7 days of culture under static conditions (glass and microdevice glass) and under flow conditions (flow rates of 30 and 50 μl/min) with the use of gelatin film as a substrate, in the presence of osteogenic medium.*

Possible mechanisms for the increased collagen production in the extracellular matrix include the exposure of the seeded cells to fluid shear, which induces mechanical stimulation and the reduction of potential nutrient transport limitations experienced by the cells cultured under static conditions.

5. Conclusions

We employed gelatin films and a fibrous collagen network as substrates for the cells and investigated the rheological properties of collagen gel. The pre-osteoblastic cells attached strongly and showed an osteogenic response inside the microfluidic system. Under both flow rates of 30 and 50 μl/min, cells appeared to be oriented along the direction of flow after 3 days of perfusion, whereas cells depicted a random orientation under static conditions. Using gelatin film as a substrate, the normalized alkaline phosphatase (ALP) activity was similar between static and flow conditions, except the flow rate of 100 μl/min, which was lower probably due to the detachment of cells under this high flow. Moreover, the collagen produced in the extracellular matrix under flow rates of 30 and 50 μl/min increased 2.2-fold and 4.4-fold, respectively, compared to static conditions. Using collagen fiber networks as a cell substrate, the ALP activity increased 1.6-fold under a flow rate of 30 μl/min compared to static ones. Additionally, the cell proliferation increased 2.4-fold under a flow rate of 50 μl/min compared to static conditions.

The increased proliferation and differentiation of pre-osteoblastic cells is attributed to the improved nutrient supply, the effective waste removal of cell metabolic products, and to the stimulation of the seeded cells through their exposure to fluid shear forces.

These findings are promising for the cell growth and the osteogenic response of pre-osteoblastic cells demonstrating the potential of using microfluidic systems in order to reduce the time needed for the generation of autologous graft substitutes which could be readily implanted in the defect site of a patient, and accelerate the new bone formation and healing.

6. References

[1] Wang, Y. L., Pelham, R. J. (1998). Preparation of a flexible, porous polyacrylamide substrate for mechanical studies of cultured cells. Methods in enzymology, 298, 489-496.

[2] Kim, B. S., Putnam, A. J., Kulik, T. J., Mooney, D. J. (1998). Optimizing seeding and culture methods to engineer smooth muscle tissue on biodegradable polymer matrices.

[3] Vunjak-Novakovic, G., Obradovic, B., Martin, I., Bursac, P. M., Langer, R., Freed, L. E. (1998). Dynamic cell seeding of polymer scaffolds for cartilage tissue engineering. Biotechnology progress, 14(2), 193-202.

[4] Carrier, R. L., Papadaki, M., Rupnick, M., Schoen, F. J., Bursac, N., Langer, R., Freed, L. E., Vunjak-Novakovic, G. (1999). Cardiac tissue engineering: cell seeding, cultivation parameters, and tissue construct characterization. Biotechnology and bioengineering, 64(5), 580-589.

[5] Riesle, J., Van Blitterswijk, C. A. (1999). Static and dynamic fibroblast seeding and cultivation in porous PEO/PBT scaffolds. Journal of Materials Science: Materials in Medicine, 10(12), 773-777.

[6] Granet, C., Laroche, N., Vico, L., Alexandre, C., Lafage-Proust, M. H. (1998). Rotating-wall vessels, promising bioreactors for osteoblastic cell culture: comparison with other 3D conditions. Medical and Biological Engineering and Computing, 36(4), 513-519.

[7] Leclerc, E., David, B., Griscom, L., Lepioufle, B., Fujii, T., Layrolle, P., Legallaisa, C. (2006). Study of osteoblastic cells in a microfluidic environment.Biomaterials, 27(4), 586-595.

[8] Yu, X., Botchwey, E. A., Levine, E. M., Pollack, S. R., & Laurencin, C. T. (2004). Bioreactor-based bone tissue engineering: the influence of dynamic flow on osteoblast phenotypic expression and matrix mineralization. Proceedings of the National Academy of Sciences of the United States of America, 101(31), 11203-11208.

[9] Bancroft, G. N., Sikavitsas, V. I., van den Dolder, J., Sheffield, T. L., Ambrose, C. G., Jansen, J. A., Mikos, A. G. (2002). Fluid flow increases mineralized matrix deposition in 3D perfusion culture of marrow stromal osteoblasts in a dose-dependent manner. Proceedings of the National Academy of Sciences, 99(20), 12600-12605.

[10] Sikavitsas, V. I., Bancroft, G. N., Holtorf, H. L., Jansen, J. A., Mikos, A. G. (2003). Mineralized matrix deposition by marrow stromal osteoblasts in 3D perfusion culture increases with increasing fluid shear forces. Proceedings of the National Academy of Sciences, 100(25), 14683-14688.

[11] Rehfeldt, F., Engler, A. J., Eckhardt, A., Ahmed, F., Discher, D. E. (2007). Cell responses to the mechanochemical microenvironment—implications for regenerative medicine and drug delivery. Advanced drug delivery reviews,59(13), 1329-1339.

[12] Vanderhooft, J. L., Alcoutlabi, M., Magda, J. J., Prestwich, G. D. (2009). Rheological Properties of Cross-Linked Hyaluronan–Gelatin Hydrogels for Tissue Engineering. Macromolecular bioscience, 9(1), 20-28.

[13] Ghosh, K., Pan, Z., Guan, E., Ge, S., Liu, Y., Nakamura, T., Ren, X., Rafailovich, M., Clark, R. A. (2007). Cell adaptation to a physiologically relevant ECM mimic with different viscoelastic properties. Biomaterials, 28(4), 671-679.
[14] Pelham, R. J., Wang, Y. L. (1998). Cell locomotion and focal adhesions are regulated by the mechanical properties of the substrate. Biological Bulletin, 348-350.
[15] Discher, D. E., Janmey, P., Wang, Y. L. (2005). Tissue cells feel and respond to the stiffness of their substrate. Science, 310(5751), 1139-1143.
[16] Mitragotri, S., Lahann, J. (2009). Physical approaches to biomaterial design.Nature materials, 8(1), 15-23.
[17] Yeung, T., Georges, P. C., Flanagan, L. A., Marg, B., Ortiz, M., Funaki, M., Zahir, N., Ming, W., Weaver, M., Janmey, P. A. (2005). Effects of substrate stiffness on cell morphology, cytoskeletal structure, and adhesion. Cell motility and the cytoskeleton, 60(1), 24-34.
[18] Pelham, R. J., Wang, Y. L. (1997). Cell locomotion and focal adhesions are regulated by substrate flexibility. Proceedings of the National Academy of Sciences, 94(25), 13661-13665.
[19]
https://boulder.research.yale.edu/Boulder-2012/Lectures/Kumacheva/Lecture_Boulder.pdf
[20] Novo, P., Volpetti, F., Chu, V., Conde, J. P. (2013). Control of sequential fluid delivery in a fully autonomous capillary microfluidic device. Lab on a Chip,13(4), 641-645.
[21] Gómez-Sjöberg, R., Leyrat, A. A., Pirone, D. M., Chen, C. S., Quake, S. R. (2007). Versatile, fully automated, microfluidic cell culture system. Analytical chemistry, 79(22), 8557-8563.
[22] Whitesides, G. M. (2006). The origins and the future of microfluidics. Nature,442(7101), 368-373.
[23] Mehling, M., Tay, S. (2014). Microfluidic cell culture. Current opinion in biotechnology, 25, 95-102.
[24] http://www.materials.uoc.gr/el/grad/courses/METY504
[25] Stevens, B., Yang, Y., Mohandas, A., Stucker, B., Nguyen, K. T. (2008). A review of materials, fabrication methods, and strategies used to enhance bone regeneration in engineered bone tissues. Journal of Biomedical Materials Research Part B: Applied Biomaterials, 85(2), 573-582.
[26] Salgado, A. J., Coutinho, O. P., Reis, R. L. (2004). Bone tissue engineering: state of the art and future trends. Macromolecular bioscience, 4(8), 743-765.
[27] Nimni, M. E., Cheung, D., Strates, B., Kodama, M., Sheikh, K. (1987). Chemically modified collagen: a natural biomaterial for tissue replacement.Journal of Biomedical Materials Research, 21(6), 741-771.
[28] Grinnell, F. (2003). Fibroblast biology in three-dimensional collagen matrices.Trends in cell biology, 13(5), 264-269.
[29] Daley, W. P., Peters, S. B., Larsen, M. (2008). Extracellular matrix dynamics in development and regenerative medicine. Journal of cell science,121(3), 255-264.

[30] Gefen, A. (2011). Cellular and Biomolecular Mechanics and Mechanobiology. Springer.
[31] Pedersen, J. A., Swartz, M. A. (2005). Mechanobiology in the third dimension. Annals of biomedical engineering, 33(11), 1469-1490.
[32] http://www.lsbu.ac.uk/water/hyrhe.html
[33] http://www.dspbio.co.jp/pdf/datasheet/ec99072810.pdf
[34] Sudo, H., Kodama, H. A., Amagai, Y., Yamamoto, S., Kasai, S. (1983). In vitro differentiation and calcification in a new clonal osteogenic cell line derived from newborn mouse calvaria. The Journal of cell biology, 96(1), 191-198.
[35] Sugawara, Y., Suzuki, K., Koshikawa, M., Ando, M., Iida, J. (2002). Necessity of enzymatic activity of alkaline phosphatase for mineralization of osteoblastic cells. Japanese journal of pharmacology, 88(3), 262-269.
[36] Hiroh, I., Masato, Y., Ryo, T., Tomoyuki, M., Tetsuo, O. (1976). Studies on phosphatidylinositol phosphodiesterase (phospholipase C type) of Bacillus cereus: I. purification, properties and phosphatase-releasing activity.Biochimica et Biophysica Acta (BBA)-Lipids and Lipid Metabolism, 450(2), 154-164.
[37] Low, M. G., Zilversmit, D. B. (1980). Role of phosphatidylinositol in attachment of alkaline phosphatase to membranes. Biochemistry, 19(17), 3913-3918.
[38] Hooper, N. M., Turner, A. J. (1988). Ectoenzymes of the kidney microvillar membrane aminopeptidase P is anchored by a glycosyl-phosphatidylinositol moiety. FEBS letters, 229(2), 340-344.
[39] Harris, H. (1990). The human alkaline phosphatases: what we know and what we don't know. Clinica Chimica Acta, 186(2), 133-150.
[40] Low, M. G., Saltiel, A. R. (1988). Structural and functional roles of glycosyl-phosphatidylinositol in membranes. Science, 239(4837), 268-275.
[41] Farley, J. R., Hall, S. L., Herring, S., Libanati, C., Wergedal, J. E. (1993). Reference standards for quantification of skeletal alkaline phosphatase activity in serum by heat inactivation and lectin precipitation. Clinical chemistry, 39(9), 1878-1884.
[42] Farley, J. R., Jorch, U. M. (1983). Differential effects of phospholipids on skeletal alkaline phosphatase activity in extracts, in situ and in circulation.Archives of biochemistry and biophysics, 221(2), 477-488.
[43] http://www.news-medical.net/health/Collagen-What-is-Collagen.aspx
[44] http://www.news-medical.net/health/Collagen-Molecular-Structure.aspx
[45] Dolomite catalogue_2012_download_0512.pdf
[46] http://www.elveflow.com/microfluidic-flow-control-products/high-accuracy-pressure-pumps
[47] http://www.elveflow.com/microfluidic-flow-control-products/microfluidic-liquid-mass-flow-sensors
[48] http://www.sensirion.com/en/technology/liquid-flow/
[49] Structural analysis of reconstituted collagen type I-Heparin Cofibrils.pdf

[50] Chatzinikolaidou, M., Lichtinger, T. K., Müller, R. T., Jennissen, H. P. (2010). Peri-implant reactivity and osteoinductive potential of immobilized rhBMP-2 on titanium carriers. Acta biomaterialia, 6(11), 4405-4421.
[51] Peter, S. J., Liang, C. R., Kim, D. J., Widmer, M. S., Mikos, A. G. (1998). Osteoblastic phenotype of rat marrow stromal cells cultured in the presence of dexamethasone, β-glycerolphosphate, and L-ascorbic acid. Journal of cellular biochemistry, 71(1), 55-62.
[52] Neto, C., Hernandes, A., Queiroz, K. C., Milani, R., Paredes-Gamero, E. J., Justo, G. Z., Peppelenbosch, M. P., Ferreira, C. V. (2011). Profiling the changes in signaling pathways in ascorbic acid/β-glycerophosphate-induced osteoblastic differentiation. Journal of cellular biochemistry, 112(1), 71-77.
[53] Chung, C. H., Golub, E. E., Forbes, E., Tokuoka, T., & Shapiro, I. M. (1992). Mechanism of action of β-glycerophosphate on bone cell mineralization.Calcified tissue international, 51(4), 305-311.
[54] Harada, S. I., Matsumoto, T., Ogata, E. (1991). Role of ascorbic acid in the regulation of proliferation in osteoblast-like MC3T3-El cells. Journal of Bone and Mineral Research, 6(9), 903-908.
[55] Franceschi, R. T., Iyer, B. S. (1992). Relationship between collagen synthesis and expression of the osteoblast phenotype in MC3T3-E1 cells.Journal of Bone and Mineral Research, 7(2), 235-246.
[56] Quarles, L. D., Yohay, D. A., Lever, L. W., Caton, R., Wenstrup, R. J. (1992). Distinct proliferative and differentiated stages of murine MC3T3-E1 cells in culture: An in vitro model of osteoblast development. Journal of Bone and Mineral Research, 7(6), 683-692.
[57] Polymers_Dilute_Solutions_Viscosity_DMA_4100.pptx
[58] Vennemann, P., Lindken, R., Westerweel, J. (2007). In vivo whole-field blood velocity measurement techniques. Experiments in fluids, 42(4), 495-511.
[59] Frangos, J. A., McIntire, L. V., Eskin, S. G. (1988). Shear stress induced stimulation of mammalian cell metabolism. Biotechnology and Bioengineering,32(8), 1053-1060.
[60] Keira, S. M., Ferreira, L. M., Gragnani, A., Duarte, I. D. S., Barbosa, J. (2004). Experimental model for collagen estimation in cell culture. Acta Cirurgica Brasileira, 19, 17-22.
[61] https://www.applichem.com/fileadmin/produktinfo/a6932_de.pdf
[62] Junqueira, L. C., Bignolas, G., Brentani, R. R. (1979). Picrosirius staining plus polarization microscopy, a specific method for collagen detection in tissue sections. The Histochemical journal, 11(4), 447-455.
[63] Terzaki, K., Kissamitaki, M., Skarmoutsou, A., Fotakis, C., Charitidis, C. A., Farsari, M., Vamvakaki, M., Chatzinikolaidou, M. (2013). Pre-osteoblastic cell response on three-dimensional, organic-inorganic hybrid material scaffolds for bone tissue engineering. Journal of biomedical materials research Part A, 101(8), 2283-2294.

[64] Barnes, H. A., Hutton, J. F., Walters, K. (1989). An introduction to rheology. Elsevier.
[65] Wu, C. C., Ding, S. J., Wang, Y. H., Tang, M. J., Chang, H. C. (2005). Mechanical properties of collagen gels derived from rats of different ages.Journal of Biomaterials Science, Polymer Edition, 16(10), 1261-1275.
[66] Motte, S., Kaufman, L. J. (2013). Strain stiffening in collagen I networks.Biopolymers, 99(1), 35-46.
[67] Shibata, Y., Abiko, Y., Moriya, Y., Yoshida, W., Takiguchi, H. (1993). Effects of transforming growth factor-β on collagen gene expression and collagen synthesis level in mineralizing cultures of osteoblast-like cell line, MC3T3-E1. International journal of biochemistry, 25(2), 239-245.
[68] Kodama H., Amagai Y.. Sudo H., Kasai S. and Yamamoto S. (1981). Establishment of a clonal osteogenic cell line from newborn mouse calvaria. Jap. J. oral BioI. 23, 899-901.
[69] Swan, C. C., Lakes, R. S., Brand, R. A., Stewart, K. J. (2003). Micromechanically based poroelastic modeling of fluid flow in Haversian bone.Journal of biomechanical engineering, 125(1), 25-37.
[70] Burger, E. H., KLEIN-NULEND, J. E. N. N. E. K. E. (1999). Mechanotransduction in bone—role of the lacuno-canalicular network. The FASEB Journal, 13(9001), S101-S112.
[71] Weinbaum, S., Cowin, S. C., Zeng, Y. (1994). A model for the excitation of osteocytes by mechanical loading-induced bone fluid shear stresses. Journal of biomechanics, 27(3), 339-360.
[72] Barron, M. J., Tsai, C. J., Donahue, S. W. (2010). Mechanical stimulation mediates gene expression in MC3T3 osteoblastic cells differently in 2D and 3D environments. Journal of biomechanical engineering, 132(4), 041005.
[73] Letechipia, J. E., Alessi, A., Rodriguez, G., Asbun, J. (2010). Would increased interstitial fluid flow through in situ mechanical stimulation enhance bone remodeling?. Medical hypotheses, 75(2), 196-198.
[74] Hillsley, M. V., Frangos, J. A. (1994). Review: Bone tissue engineering: The role of interstitial fluid flow. Biotechnology and bioengineering, 43(7), 573-581.
[75] Alenghat, F. J., Ingber, D. E. (2002). Mechanotransduction: all signals point to cytoskeleton, matrix, and integrins. Sci STKE, 119(6).
[76] van den Dolder, J., Bancroft, G. N., Sikavitsas, V. I., Spauwen, P. H., Jansen, J. A., Mikos, A. G. (2003). Flow perfusion culture of marrow stromal osteoblasts in titanium fiber mesh. Journal of biomedical materials research Part A, 64(2), 235-241.
[77] Holtorf, H. L., Jansen, J. A., Mikos, A. G. (2005). Flow perfusion culture induces the osteoblastic differentiation of marrow stromal cell-scaffold constructs in the absence of dexamethasone. Journal of Biomedical Materials Research Part A, 72(3), 326-334.
[78] Sikavitsas, V. I., Bancroft, G. N., Lemoine, J. J., Liebschner, M. A., Dauner, M., Mikos, A. G. (2005). Flow perfusion enhances the calcified matrix deposition of

marrow stromal cells in biodegradable nonwoven fiber mesh scaffolds. Annals of biomedical engineering, 33(1), 63-70.
[79] Gomes, M. E., Sikavitsas, V. I., Behravesh, E., Reis, R. L., Mikos, A. G. (2003). Effect of flow perfusion on the osteogenic differentiation of bone marrow stromal cells cultured on starch-based three-dimensional scaffolds. Journal of Biomedical Materials Research Part A, 67(1), 87-95.
[80] Lian, J. B., Stein, G. S. (1992). Concepts of osteoblast growth and differentiation: basis for modulation of bone cell development and tissue formation. Critical Reviews in Oral Biology & Medicine, 3(3), 269-305.
[81] Glowacki, J., Mizuno, S., Greenberger, J. S. (1998). Perfusion enhances functions of bone marrow stromal cells in three-dimensional culture. Cell transplantation, 7(3), 319-326.